Indonesian Journal of Biotechnology

VOLUME 29(1), 2024, 25-32 | RESEARCH ARTICLE

Protective effects of *Zingiber cassumunar* Roxb. extract against UVB-induced oxidative stress in Wistar albino rats (*Rattus novergicus* Berkenhout, 1769)

Dian Ayuning Tyas[1], Nastiti Wijayanti[2], Tri Rini Nuringtyas[3,*], Subagus Wahyuono[4]

[1]Doctoral Program of Biotechnology, Graduate School, Universitas Gadjah Mada, Yogyakarta 55281, Indonesia
[2]Department of Tropical Biology, Faculty of Biology, Universitas Gadjah Mada, Yogyakarta 55281, Indonesia
[3]Biotechnology Research Center, Universitas Gadjah Mada, Yogyakarta 55281, Indonesia
[4]Department of Pharmaceutical Biology, Faculty of Pharmacy, Universitas Gadjah Mada, Yogyakarta 55281, Yogyakarta
*Corresponding author: tririni@ugm.ac.id

SUBMITTED 28 October 2023 **REVISED** 5 December 2023 **ACCEPTED** 8 December 2023

ABSTRACT Protecting the skin from the effects of UVB radiation using natural products is crucial in the cosmeceutical industry. This study aims to investigate the protective effects of Bangle (*Zingiber cassumunar* Roxb.) against UVB-induced skin damage in Wistar albino rats. The rhizomes were macerated using 70% ethanol v/v, followed by n-hexane to obtain n-hexane soluble and n-hexane insoluble fraction. The antioxidant properties of the ethanol extracts and n-hexane soluble fraction were evaluated using a 2,2-diphenyl-1-picrylhydrazyl (DPPH) assay. The study also examined the antiphotoaging properties through reactive oxygen species (ROS) scavenging assay, matrix metalloproteinase-1 (*MMP-1*) expression, and tyrosinase expression against UVB radiation in Wistar albino rats. The results demonstrated that the *Z. cassumunar* extract and fraction effectively converted DPPH radicals into a more stable compound. Analysis revealed the presence of Benzene, 4-(1Z)-1,3-butadien-1-yl-1,2-dimethoxy- and (E)-4-(3,4-Dimethoxyphenyl) but-3-en-1-ol as the primary compounds in both the extract and fraction, suggesting their contribution to the observed activity. Furthermore, *Z. cassumunar* compounds could reduce UVB-induced ROS production and may protect against skin photoaging by changing the expression of *MMP-1* and tyrosinase levels in Wistar albino rats. These findings suggest that *Z. cassumunar* holds promise for preventing skin aging.

KEYWORDS Matrix metalloproteinase; Skin photoaging; Ultraviolet B; *Zingiber cassumunar*

1. Introduction

The skin is an essential barrier organ that protects organs from the external environment, such as chemical and physical stimuli, microorganisms, and sunlight (Shin 2020). Among the threads above, sunlight has a severe impact on the skin. Excessive exposure to sunlight, particularly ultraviolet (UV) B radiation, leads to sunburn and oxidative stress. These can result in skin damage, such as premature aging, inflammation, and tumor growth (Albrecht et al. 2019; Kwon et al. 2019). UVB radiation has the ability to directly induce DNA degradation within cellular structures and cause reactive oxygen species (ROS). The excessive presence of ROS leads to the decreasing quality of collagen, the extracellular matrix, and elastin. Additionally, they induce the synthesis of matrix metalloproteinases (MMPs) and proteolytic enzymes, resulting in the degradation of protein fibers. Matrix metalloproteinase-1 (*MMP-1*) is also known to exert a critical function in the degradation process of fibrillary collagens. Consequently, increased ROS production modifies skin collagen during aging, leading to skin wrinkles and a reduction in elasticity (Lephart 2016).

Melanin, generated by melanocytes, is the primary component of skin pigmentation. UVB exposure is usually blocked by normal melanin synthesis from causing skin damage. Melanocyte-stimulating hormone (MSH) is an essential intrinsic agent that stimulates melanogenesis. It increases the production of melanin and microphthalmia-associated transcription factor (MITF), and MSH promotes cAMP response element-binding protein (CREB). MITF is a melanogenesis regulator that binds to tyrosinase. Thus, the key melanogenic components that MITF regulates transcription are tyrosinase, tyrosinase-related protein-1 (TRP-1), and TRP-2 (Kim et al. 2020).

Plants protect themselves from UV radiation by producing secondary metabolites that have the ability for that purpose. The secondary metabolites product also preserves the skin from photoaging (Petruk et al. 2018). Several studies have been undertaken to identify phytochemicals that might enhance the antioxidant defense system to

delay skin aging. Bangle (*Zingiber cassumunar* Roxb.) is classified as an herbaceous perennial plant species characterized by the presence of subterranean rhizomes. Gastrointestinal diseases, respiratory problems, and inflammation used to be treated using Bangle as a medicinal herb in Thailand, Indonesia, and other Asian countries (Chongmelaxme et al. 2017). This rhizome is known to contain a diverse range of chemical compounds, such as phenylbutenoids, sesquiterpenoids, curcuminoids, phenolics, benzaldehydes, and essential oils that consist of monoterpenoids (Han et al. 2021). However, there is a scarcity of research on the possible application of Bangle as a natural sunscreen agent. This study aimed to investigate the antioxidant characteristics of *Z. cassumunar* and assess its ability to reduce UVB-induced oxidative stress in Wistar albino rats through the analysis of ROS, the expression level of matrix metalloproteinase-1 (*MMP-1*), and tyrosinase genes.

2. Materials and Methods

2.1. Plant material and extract preparation

Zingiber cassumunar Roxb. rhizomes were obtained from Karanganyar, Central Java, Indonesia, and examined at the Laboratory of Plant Systematic, Faculty of Biology, Universitas Gadjah Mada, with specimen certificate 014583/S. Tb/IV/2019. The rhizomes of Bangle were cleaned and set to be dried using the oven at 50 °C. Approximately 60 g powdered rhizomes were macerated overnight in 300 mL ethanol (70% v/v) and filtered using Whatman filter paper No.1. The ethanol extract was dried using a rotary evaporator at 40 °C. The ethanol extract was mixed with n-hexane, forming a soluble n-hexane fraction and an insoluble n-hexane fraction to differentiate the extract into nonpolar and polar components. The secondary metabolites were assessed using Thin Layer Chromatography (TLC) with silica gel F_{254} as the stationary phase and n-hexane-ethyl acetate (4:1 v/v) as the mobile phase. $Ce(SO_4)_2$ is a universal detection reagent for organic compounds, consisting of concentrated sulfuric acid and acetic anhydrite, which have degradative and oxidative properties (Susilo and Suciati 2016). Therefore, TLC profiles were observed under UV_{254} and UV_{366} light as well as spray reagent $Ce(SO_4)_2$. After elution with the mobile phase, a reagent of 2,2-diphenyl-1-picrylhydrazyl (DPPH) was used to spray the TLC plate for the autobiography of spots with antioxidant activity. The positive spot was scraped from the TLC, re-extracted with the same solvent, and fractionated using vacuum liquid chromatography (VLC).

2.2. Metabolite profiling using gas chromatography-mass spectrometer (GC-MS)

This study performed metabolite analysis profiling using the method of Bin Jantan et al. (2003) with a slight modification. TRACE™ 1310 GC (Thermo, USA) was used for the GC-MS analysis. This GC-MS system is fitted with a TG-5MS silica capillary column (30 m × 0.25 mm; 0.25 µm thickness) with the following temperature gradient 75 °C to 230 °C at 3 °C/min at a linear velocity of 50 cm/s. A flow rate was 1 m/min with a split injection 1:10 ratio. The injector and detector temperature were programmed at 250 °C. The chemical components were identified using their mass spectral data compared to the available Wiley library, measured retention indices with literature values, and co-chromatography for certain constituents in the capillary column containing authentic components.

2.3. In vitro antioxidant assay

The free radical scavenging method is used in this study to determine antioxidant assay using the 2,2-diphenyl-1-picrylhydrazyl (DPPH) (Wulansari et al. 2016). DPPH 0.004% was used in this study, while ascorbic acid was used as a standard. The absorbance of the solution was observed using a spectrophotometer at 516 nm (Shimadzu UV-1800, Japan). The antioxidant activity was calculated by using the following formula:

$$\text{DPPH scavenging effect } (\%) = 100\times\left[\frac{(Abs\ control - Abs\ sample)}{Abs\ sample}\right] \quad (1)$$

2.4. Hyperpigmentation rat model

Twenty-five male Wistar rats weighing 250 ± 25 g were fed ad libitum at room temperature 28 °C and 12 h photoperiod. The rats were classified into five groups consisting of five rats: control, UVB-irradiated control, UVB-irradiated and vehicle (PEG)-treated, UVB-irradiated and extract-treated, and UVB-irradiated and fraction-treated groups. The rats were divided into groups after a week of acclimatization. Vehicle-treated UV-B irradiated rats were topically administered by 200 µL of vehicle (PEG) daily, and the extract/fraction-treated rats were topically administered by 200 µL of 2% samples prepared in vehicle [propylene glycol: ethanol: water (5:3:2)] daily (Lee et al. 2014a). The samples were applied to the dorsal skin after UVB irradiation. Control groups did not receive any treatment. This study uses UVB light with broadband emission at 302 nm (CL-100M, UVP, USA). The rats were exposed to a UVB irradiation dose of 390 mJ/cm^2 three times a week. This treatment was conducted for two weeks. This protocol was conducted according to a previous study from You et al. (2019) with some modifications. The Ethical Committee of the Faculty of Medicine, Universitas Islam Sultan Agung, Semarang, officially accepted this protocol with certificate number 55/2/2022/Komisi Bioetik.

2.5. Measurements of reactive oxygen species (ROS) production

After 24 h of the last treatment, the rats in all groups were subsequently euthanized. The rat's blood was acquired by retro-orbital blood sampling. Blood samples from Wistar albino rats were marked with 30 µM 2′,7′-dichlorofluorescein diacetate (DCFH-DA) (Sigma-Aldrich, USA) at 37 °C for 30 min in a CO_2 incubator. Flow cytometry (FACSCalibur™; Becton-Dickinson,

TABLE 1 Primer sequences (Zukhiroh et al. 2022).

Gene	Forward sequences	Reverse sequences
GADPH	5'-CATGGCCTTCCGTGTTCCTA-3'	5'-GCGGCACGRCAGATCCA-3'
MMP-1	5'-GACCGTTCTATTCCTCAGTGCAA-3'	5'-CCCGGTGACACACAAAGACA-3'
tyr	5'-GAATGGAACAATGTCCCAAG-3'	5'-CCTTCGCAGCCATTGTTC-3'

USA) was used to analyze ROS production.

2.6. MMP-1 and tyrosinase (tyr) expression

The study of *MMP-1* and tyrosinase (*tyr*) expression was analyzed using the method developed by Zukhiroh et al. (2022). TRIzol (Invitrogen, China) was used to extract Total RNA from the skin tissue of Wistar rats. Super-Script II was used to synthesize the first-strand cDNA (Invitrogen, USA) with SYBR No ROX Green I dye (SMOBIO Technology Inc, Taiwan) used as reverse transcription. rt-PCR process was set up with an initial step at 95 °C for 10 min, 95 °C for 15 s, and 60 °C for 1 min. The respective primers (Table 1) were used to measure the mRNA levels of *MMP-1* and tyrosinase (*tyr*). Later, Eco Software v5.0 (Illumina Inc, USA) was used to analyze previously obtained data.

3. Results and Discussion

3.1. Extraction of Z. cassumunar

The process of extracting dried *Z. cassumunar* rhizomes yielded 14.3 g of extract, with a yield efficiency of 24.23%. The visible look of the extract was characterized by a glossy, brown, and moist aspect, which can be attributed to its essential oil composition. The TLC profiles set out differences in the chemicals present within the fractions, as shown in Figure 1. Most compounds exhibited quenching in the UV_{254} region. Upon visualization with $Ce(SO_4)_2$, they displayed a red-brown coloration, possibly associated with an unsaturated double bond in the chemical (Fadhilah et al. 2021). Blue fluorescence spots under UV_{366} suggested an aromatic ring or phenolic compound's presence.

3.2. GC-MS analysis of metabolite profiling

GC-MS analysis further processed ethanol extract and n-hexane fraction to identify bioactive compounds. Several compounds were shown after GC-MS had been conducted (Figure 2). A total of six phytochemicals were found as elements of the extract, whereas four major phytochemicals were identified as constituents of the fraction, as indicated in Table 2. Both compounds, namely 4-(1Z)-1,3-butadien-1-yl-1,2-dimethoxybenzene (21.65 min) and (E)-4-(3,4-Dimethoxyphenyl) but-3-en-1-yl acetate (29.12 min), are present as the primary component. Both extract and fraction contained (E)-4-(But-1-en-1-yl)-1,2-dimethoxybenzene and (E)-4-(3,4-Dimethoxyphenyl with different peak area percentages. Masuda and Jitoe (1995) stated that the phenylbutanoids groups detected in *Z. cassumunar* have analgesic, anti-inflammatory, and antioxidative activities. According to the data presented in Table 2, it could be assumed that terpinen 4-ol (10.41 min) was exclusively identified from the extract. Terpinen 4-ol is one of the antimicrobial and antioxidant monoterpenes of *Z. cassumunar* (Sukatta et al. 2009). Based on the findings, the compounds mentioned previously might serve as the primary constituents with anti-aging properties in *Z. cassumunar* rhizome.

3.3. DPPH radical scavenging assay

The free radical scavenging activities of the samples The DPPH were determined using scavenging assay. Extract of *Z. cassumunar* significantly scavenged DPPH radical with the IC_{50} value of 74.28 µg/mL, and it is more significant than the fraction with the IC_{50} value of 169.33 µg/mL. Both extract and fraction could convert DPPH radicals into species that have more stability (DPPH-H or DPPH-R). In this study, positive control showed the IC_{50} value of 38.93 µg/mL. This activity was influenced by a phenolic derivative compound, which contributes to reducing free radicals by donating their protons (Nur et al. 2019).

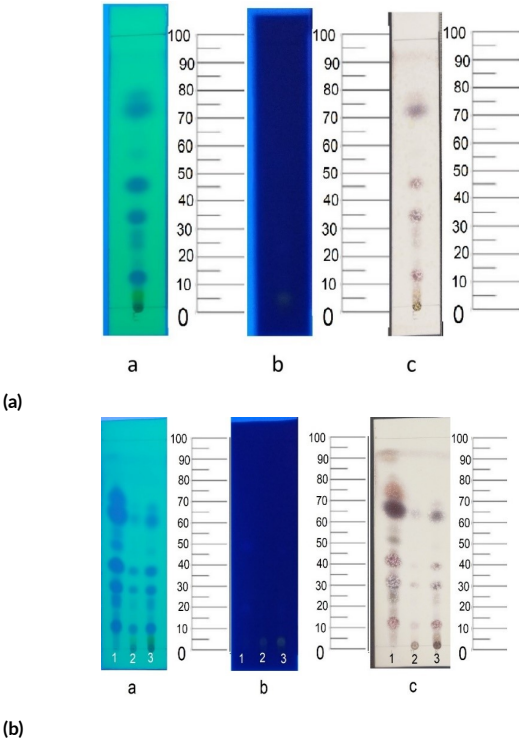

FIGURE 1 TLC profile fractions visualized by UV_{254} (a), UV_{366} (b), $Ce(SO_4)_2$ (c). Stationary phase using silica gel F_{254} with mobile phase n-hexane: ethyl acetate 4:1 (v/v).

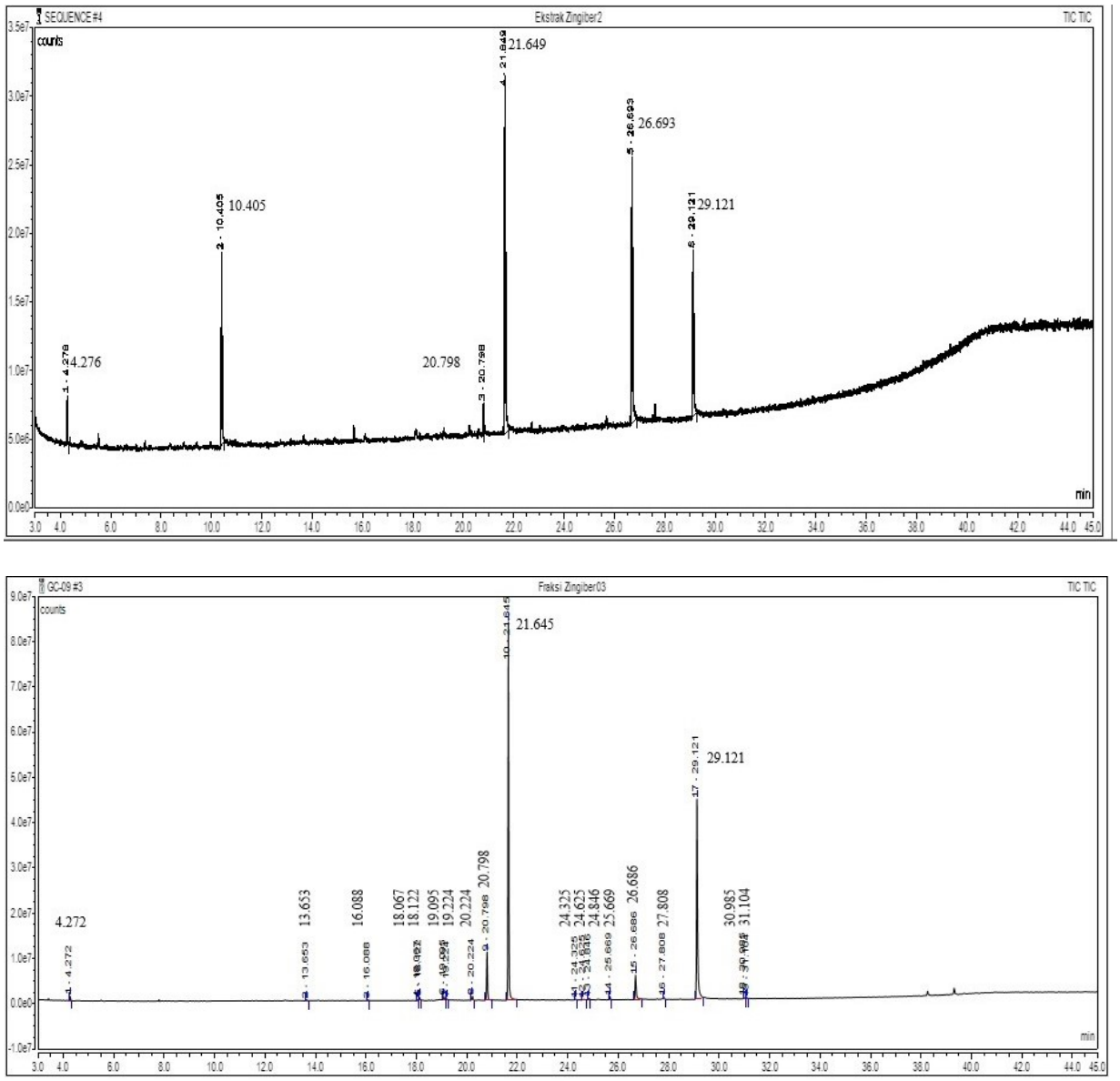

FIGURE 2 GC-MS chromatogram of (a) extract and (b) fraction of *Zingiber cassumunar* Roxb.

3.4. Measurements of ROS Production

Figure 3 demonstrates that the n-hexane fraction and ethanol extract of *Z. cassumunar* have the ability to reduce the effect of ROS caused by UVB radiation. In comparison to the production of 53.4% of ROS by the UV irradiated control group, the ethanol extract showed a reduction of 15.7% and the n-hexane fraction showed a reduction of 6.6%. The observation of reactive oxygen species (ROS) is accomplished by measuring 2′,7′-dichlorofluorescein diacetate (DCFH-DA) to 2′-7′dichlorofluorescein (DCF) that conducted an oxidation reaction. The cellular uptake of DCFH-DA involves the enzymatic cleavage of acetyl groups by cellular esterase, causing the formation of DCFH. The molecule DCFH underwent oxidation by ROS, causing conversion of the molecule to DCF. This conversion led to the emission of fluorescence that excites an emission wavelength of 485 nm and 530 nm, commonly visualized as green fluorescence (Kim and Xue 2020).

3.5. MMP-1 and tyrosinase expression

To explain the molecular mechanism that mediates the protection of *Z. cassumunar* against photo-aging, gene expression changes of *MMP-1* and tyrosinase were measured (Figure 4). These results suggested that *Z. cassumunar* extract and fraction showed a comparable *MMP-1* relative expression while the fraction showed a significantly higher tyrosinase (*tyr*) gene expression compared with the extract.

3.6. Discussion

Due to synthetic medications' adverse effects, research on natural products potentially extending human lifetimes

TABLE 2 Comparison of GC-MS results of extract and fraction of *Zingiber cassumunar* Roxb.

Extract				Fraction			
Peak no.	**R.T. (min)**	**Compound Name**	**Peak Area (%)**	**Peak no.**	**R.T. (min)**	**Compound Name**	**Peak Area (%)**
1.	4.28	Ethane, 1,1,2,2-tetrachloro-	2.66	1.	4.27	Ethane, 1,1,2,2-tetrachloro-	0.41
2.	10.41	Terpinen-4-ol	17.01	2.	13.65	Methyl 10,12-octadecadiynoate	0.25
3.	20.80	(E)-4-(But-1-en-1-yl)-1,2-dimethoxybenzene	2.50	3.	16.09	3,5-Dimethoxyamphetamine	0.16
4.	**21.65**	**Benzene, 4-(1Z)-1,3-butadien-1-yl-1,2-dimethoxy-**	**33.70**	4.	18.07	Methyl 3,5-tetradecadiynoate	0.22
5.	**26.69**	**(E)-4-(3,4-Dimethoxyphenyl)but-3-en-1-ol**	**27.00**	5.	18.12	Benzaldehyde, 3,4-dimethoxy-	0.54
6.	**29.12**	**(E)-4-(3,4-Dimethoxyphenyl)but-3-en-1-yl acetate**	**17.14**	6.	19.09	(Z)-4-(but-1-en-1-yl)-1,2-dimethoxybenzene	0.44
				7.	19.22	Benzeneethanamine, 2,5-difluoro-ß,3,4-trihydroxy-N-methyl-	0.21
				8.	20.22	Benzene, 4-(1Z)-1,3-butadien-1-yl-1,2-dimethoxy-	0.59
				9.	20.80	(E)-4-(But-1-en-1-yl)-1,2-dimethoxybenzene	6.78
				10.	**21.65**	**Benzene, 4-(1Z)-1,3-butadien-1-yl-1,2-dimethoxy-**	**49.55**
				11.	24.33	Benzeneethanamine, 2,5-difluoro-ß,3,4-trihydroxy-N-methyl-	0.18
				12.	24.62	(Z)-1-(2,4,5-Trimethoxyphenyl)but-1-ene	0.20
				13.	24.85	2-Propenal, 3-(3,4-dimethoxyphenyl)-	0.32
				14.	25.67	(Z)-1-(Buta-1,3-dien-1-yl)-2,4,5-trimethoxybenzene	0.52
				15.	26.69	(E)-4-(3,4-Dimethoxyphenyl)but-3-en-1-ol	4.67
				16.	27.81	Methyl 3-methyl-pentadecanoate	0.29
				17.	**29.12**	**(E)-4-(3,4-Dimethoxyphenyl)but-3-en-1-yl acetate**	**34.18**
				18.	30.98	Methyl 9-cis,11-trans-octadecadienoate	0.26
				19.	31.10	Benzeneethanamine, 2,5-difluoro-ß,3,4-trihydroxy-N-methyl-	0.24

Note: Bold font indicates the phytochemicals with the high peak area percentages.

has increased. In cosmeceuticals, protecting skin from UVB rays with natural products is critical. Asian perennial herbaceous rhizomes, *Z. cassumunar*, are examined for antioxidant and anti-melanogenic effects. Antioxidant function reduces oxidative damage, preventing inflammation and aging. Developing anti-aging properties requires screening natural compounds for free radical scavenging. *Z. cassumunar* compound converted DPPH radicals to more stable species in this investigation.

According to the GC-MS analysis, *Z. cassumunar* contains benzene, 4-(1Z)-1,3-butadiene-1-yl-1,2-dimethoxy- as the main component. This phenylbutanoic component is related to anti-inflammatory properties. As stated previously, skin inflammation could be caused by excessive UV radiation. These results can be compared to previous research. The inflammatory responses are related to melanin synthesis. (E)-4-(3,4-Dimethoxyphenyl) but-3-en-1-ol could enhance melanin synthesis in B16F10 melanoma cells by up-regulating tyrosinase expression. Tyrosinase activity increases due to the increasing tyrosinase levels after (E)-4-(3,4-Dimethoxyphenyl) but-3-en-1-ol- treated in B16F10 melanoma cells (Park et al. 2015). Tyrosinase is the main enzyme in melanogenesis and is involved in the conversion process of tyrosine to L-DOPA, which is converted to dopaquinone, a precursor to the synthesis of brownish 5,6-dihidroxyindole-2-carboxylic acid-rich melanin (Lee et al. 2014b).

Skin produces RO and activates various biological responses if exposed to UV radiation. Pigmentation is a normal response to prevent damage caused by UVR. Tyrosinase is a copper-containing enzyme that catalyzes pigmentation in the skin. Thus, tyrosinase acts as the key enzyme that limits melanogenesis. The first step in melanogenesis involves the catalytic reaction, and tyrosinase oxidizes

phenols to ortho-quinones. However, there is a possibility that melanogenesis involves catechol to ortho-quinones

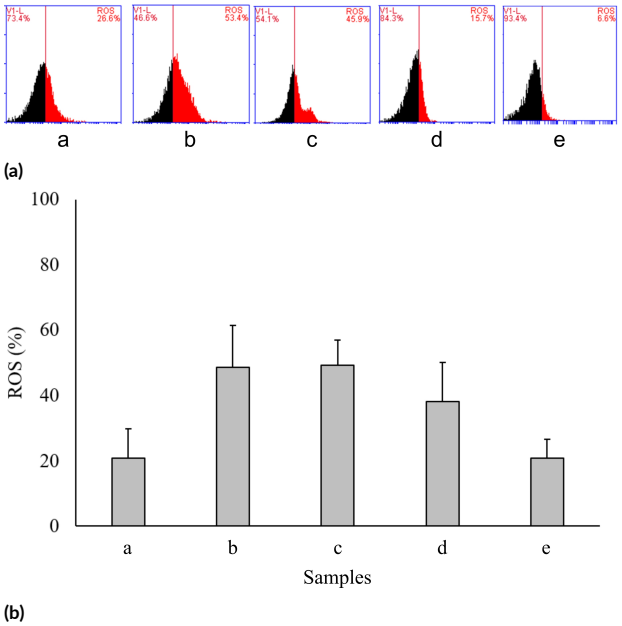

FIGURE 3 The level of ROS in *Z. cassumunar* treated as indicated for 24 h was measured using flow cytometry with DCFH-DA dye. (a) sham, (b) UVB-irradiated control, (c) UVB-irradiated and based gel (PEG), (d) UVB-irradiated and extract, (e) UVB-irradiated and fraction. The representative flow cytogram is depicted in the upper panel, while the lower panel is the quantification of the ROS level.

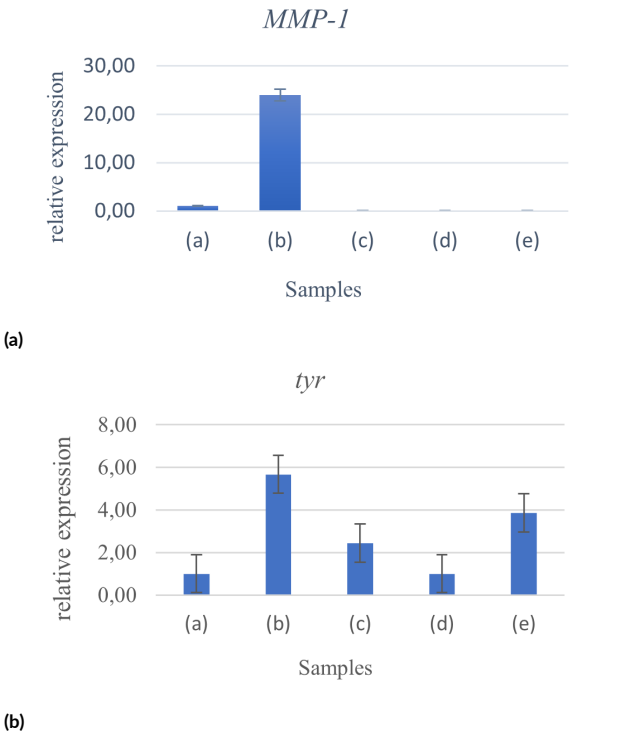

FIGURE 4 MMP-1 and tyrosinase (tyr) relative expression levels after treatment were determined by reverse transcription-PCR using GADPH as an internal control. (a) sham, (b) UVB-irradiated control, (c) UVB-irradiated and based gel (PEG), (d) UVB-irradiated and extract, (e) UVB-irradiated and fraction.

alongside the catalytic reaction. Wang et al. (2018) report that there is a synergistic effect between the antioxidant system and melanogenesis associated with ROS scavenging activity. The effectiveness of scavenging radical activity increases while tyrosinase inhibitors work and reduce melanin production. As a result, antioxidant effects and inhibition of melanin biosynthesis are shown by plants containing phenolic compounds reducing the substances that induce tyrosinase.

Wrinkle formation is known to be promoted by *MMP-1* caused by decomposing collagen type-1. In the skin, collagen type-1 and *MMP-1* activity synthesis are balanced. Promoting collagen production is considered a way of preventing aging (Lee et al. 2023). However, due to environmental causes, synthesis of collagen type-1 is lower, and *MMP-1* activity is increased while aging. UV irradiation, one of the environmental causes, could profoundly impact the regulation of ROS formation and, thus, is possibly mediated by the attenuation of the *MMP-1* production, which leads to collagen fragmentation and decreased collagen synthesis (Shin et al. 2019). The findings of this study indicate that the secondary metabolites derived from this rhizome have promising properties for use in antiphotoaging formulations, which promote the utilization of *Z. cassumunar* as a nutraceutical agent for its potential antiphotoaging properties.

4. Conclusions

Both extract and fraction of *Z. cassumunar* could convert DPPH radicals into a more stable species. The extract and fraction consisted of two primary chemicals, namely Benzene, 4-(1Z)-1,3-butadien-1-yl-1,2-dimethoxy- and (E)-4-(3,4-Dimethoxyphenyl) but-3-en-1-ol. As both were detected in fraction and extract, these compounds were identified as potential contributors to the observed activity. This study discovered evidence that *Z. cassumunar* has antioxidant properties and is capable of reducing the generation of ROS generated by UVB radiation. In summary, it could be suggested that *Z. cassumunar* has the potential to mitigate skin photo-aging through modulation of *MMP-1* and tyrosinase expression.

Acknowledgments

This study was financially supported by the Indonesian Endowment Fund for Education (LPDP). This research is part of the first author's dissertation.

Authors' contributions

DAT, NW, TRN, and SW designed the study. DAT, SW carried out the laboratory work. DAT, NW, TRN, and SW analyzed the data. DAT, NW, and TRN wrote the manuscript. All authors read and approved the final version of the manuscript.

Competing interests

The authors declare no conflict of interest in this study.

References

Albrecht S, Jung S, Müller R, Lademann J, Zuberbier T, Zastrow L, Reble C, Beckers I, Meinke MC. 2019. Skin type differences in solar-simulated radiation-induced oxidative stress. Br. J. Dermatol. 180(3):597–603. doi:10.1111/bjd.17129.

Bin Jantan I, Mohd Yassin MS, Chin CB, Chen LL, Sim NL. 2003. Antifungal activity of the essential oils of nine Zingiberaceae species. Pharm. Biol. 41(5):392–397. doi:10.1076/phbi.41.5.392.15941.

Chongmelaxme B, Sruamsiri R, Dilokthornsakul P, Dhippayom T, Kongkaew C, Saokaew S, Chuthaputti A, Chaiyakunapruk N. 2017. Clinical effects of *Zingiber cassumunar* (Plai): A systematic review. Complement. Ther. Med. 35:70–77. doi:10.1016/j.ctim.2017.09.009.

Fadhilah K, Wahyuono S, Astuti P. 2021. Fractions and isolated compounds from *Lansium domesticum* fruit peel exhibited cytotoxic activity against T-47D and HepG2 cell lines. Biodiversitas 22:3743–3748. doi:10.13057/biodiv/d220918.

Han AR, Kim H, Piao D, Jung CH, Seo EK. 2021. Phytochemicals and bioactivities of *Zingiber cassumunar* Roxb. Molecules 26(8):2377. doi:10.3390/molecules26082377.

Kim H, Xue X. 2020. Detection of total reactive oxygen species in adherent cells by 2',7'-dichlorodihydrofluorescein diacetate staining. J. Vis. Exp. 2020(160):10.3791/60682. doi:10.3791/60682.

Kim JH, Lee JE, Kim T, Yeom MH, Park JS, di Luccio E, Chen H, Dong Z, Lee KW, Kang NJ. 2020. 7,3′,4′-trihydroxyisoflavone, a metabolite of the soy isoflavone daidzein, suppresses α-melanocyte-stimulating hormone-induced melanogenesis by targeting melanocortin 1 receptor. Front. Mol. Biosci. 7:577284. doi:10.3389/fmolb.2020.577284.

Kwon KR, Alam MB, Park JH, Kim TH, Lee SH. 2019. Attenuation of UVB-induced photo-aging by polyphenolic-rich *Spatholobus suberectus* stem extract via modulation of MAPK/AP-1/MMPs signaling in human keratinocytes. Nutrients 11(6):1341. doi:10.3390/nu11061341.

Lee KO, Kim SN, Kim YC. 2014a. Anti-wrinkle effects of water extracts of teas in hairless mouse. Toxicol. Res. 30(4):283–289. doi:10.5487/TR.2014.30.4.283.

Lee MS, Oh YJ, Kim JW, Han KM, Kim DS, Park JW, Kim HM, Kim DW, Kim YS. 2023. Antioxidant, whitening, antiwrinkle, and anti-inflammatory effect of *Ajuga spectabilis* Nakai extract. Plants 12(1):79. doi:10.3390/plants12010079.

Lee TH, Seo JO, Baek SH, Kim SY. 2014b. Inhibitory effects of resveratrol on melanin synthesis in ultraviolet B-induced pigmentation in guinea pig skin. Biomol. Ther. 22(1):35–40. doi:10.4062/biomolther.2013.081.

Lephart ED. 2016. Skin aging and oxidative stress: Equol's anti-aging effects via biochemical and molecular mechanisms. Ageing Res. Rev. 31:36–54. doi:10.1016/j.arr.2016.08.001.

Masuda T, Jitoe A. 1995. Phenylbutenoid monomers from the rhizomes of *Zingiber cassumunar*. Phytochemistry 39(2):459–461. doi:10.1016/0031-9422(94)00883-U.

Nur S, Mubarak F, Jannah C, Winarni DA, Rahman DA, Hamdayani LA, Sami FJ. 2019. Total phenolic and flavonoid compounds, antioxidant and toxicity profile of extract and fractions of paku atai tuber (*Angiopteris ferox* Copel). Food Res. 3(6):734–740. doi:10.26656/fr.2017.3(6).135.

Park J, Chung H, Bang SH, Han AR, Seo EK, Chang SE, Kang DH, Oh ES. 2015. (E)-4-(3,4-dimethoxyphenyl)but-3-en-1-ol enhances melanogenesis through increasing upstream stimulating factor-1-mediated tyrosinase expression. PLoS One 10(11):e0141988. doi:10.1371/journal.pone.0141988.

Petruk G, Giudice RD, Rigano MM, Monti DM. 2018. Antioxidants from plants protect against skin photoaging. Oxid. Med. Cell. Longev. 2018:1454936. doi:10.1155/2018/1454936.

Shin DW. 2020. Various biological effects of solar radiation on skin and their mechanisms: Implications for phototherapy. Animal Cells Syst. (Seoul). 24(4):181–188. doi:10.1080/19768354.2020.1808528.

Shin JW, Kwon SH, Choi JY, Na JI, Huh CH, Choi HR, Park KC. 2019. Molecular mechanisms of dermal aging and antiaging approaches. Int. J. Mol. Sci. 20(9):2126. doi:10.3390/ijms20092126.

Sukatta U, Rugthaworn P, Punjee P, Chidchenchey S, Keeratinijakal V. 2009. Chemical composition and physical properties of oil from Plai (*Zingiber cassumunar* Roxb.) obtained by hydro distillation and hexane extraction. Kasetsart J. - Nat. Sci. 43(5):212–217.

Susilo S, Suciati R. 2016. Studies of morphological and secondary metabolites variety of mosses (bryophytes) in Cibodas, West Java. Int. J. Adv. Res. (Indore) 4(12):1397–1402. doi:10.21474/IJAR01/2536.

Wang Y, Hao MM, Sun Y, Wang LF, Wang H, Zhang YJ, Li HY, Zhuang PW, Yang Z. 2018. Synergistic promotion on tyrosinase inhibition by antioxidants. Molecules 23(1):106. doi:10.3390/molecules23010106.

Wulansari ED, Wahyuono S, Marchaban, Widyarini S. 2016. Potential bengle (*Zingiber cassumunar* Roxb.) rhizomes for sunscreen and antioxidant compounds. Int. J. PharmTech Res. 9(11):72–77.

You YJ, Wu PY, Liu YJ, Hou CW, Wu CS, Wen KC, Lin CY, Chiang HM. 2019. Sesamol inhibited ultraviolet radiation-induced hyperpigmentation and damage in C57BL/6 mouse skin. Antioxidants 8(7):207.

doi:10.3390/antiox8070207.

Zukhiroh Z, Putra A, Chodidjah C, Sumarawati T, Subchan P, Trisnadi S, Hidayah N, Amalina ND. 2022. Effect of secretome-hypoxia mesenchymal stem cells on regulating SOD and MMP-1 mRNA expressions in skin hyperpigmentation rats. Open Access Maced. J. Med. Sci. 10(A):1–7. doi:10.3889/oamjms.2022.10348.